High bandwidth absorption spectroscopy with a dispersed supercontinuum source

Johan Hult*, Rosalynne S. Watt, and Clemens F. Kaminski

Department of Chemical Engineering, University of Cambridge, Pembroke Street, Cambridge CB2 3RA, UK
*Corresponding author: jfh36@cam.ac.uk

Abstract: An optical gas sensor is presented, making use of a dispersed supercontinuum source, capable of acquiring broad bandwidth spectra at ultrahigh wavelength sweep and repetition rates. Wavelength sweeps from 1100 nm to 1700 nm can be performed in 800 ns at a spectral resolution of 40 pm. This is comparable to line-widths of molecular spectra at atmospheric pressure. Quantitative measurements are presented of CH_4 employing 80 nm wide sweeps over the P- Q- and R-branches of the $2\nu_3$ transition near 1665 nm, at rates exceeding 100 kHz. The effective acquisition rate is determined by the amount of averaging required, and the effect of this averaging on observed precision is investigated.

©2007 Optical Society of America

OCIS codes: (300.6500) Spectroscopy, time-resolved; (300.1030) Absorption; (140.3600) Lasers, tunable

References and links

1. M. G. Allen, E. R. Furlong, and R. K. Hanson, "Tunable Diode Laser Sensing and Combustion Control," in *Applied Combustion Diagnostics*, K. Kohse-Hoinghaus, J. B. Jeffries eds., (Taylor & Francis, New York, 2002).
2. M. G. Allen, "Diode laser absorption sensors for gas-dynamic and combustion flows," Meas. Sci. Technol. **9**, 545-562 (1998).
3. P. A. Martin, "Near-infrared diode laser spectroscopy in chemical process and environemental air monitoring," Chem. Soc. Rev. **31**, 201-210 (2002).
4. M. Lackner, G. Totschnig, F. Winter, M. Ortsiefer, M-C. Ackman, R. Shau, and J. Rosskopf, "Demonstration of methane spectroscopy using a vertical-cavity surface-emitting laser at 1.68 µm with up to 5 MHz repetition rate," Meas. Sci. Technol. **14**, 101-106 (2003).
5. S. T. Sanders, D. W. Mattison, J. B. Jeffries, and R. K. Hanson,"Rapid temperature tuning of a 1.4-mum diode laser with application to high-pressure H_2O absorption spectroscopy," Opt. Lett. **26**, 1568-1570 (2001).
6. E. L. Normand, M. T. McCulloch, G. Duxbury, and N. Langford, "Fast, real-time spectrometer based on a pulsed quantum-cascade laser," Opt. Lett. **28**, 16-18 (2003).
7. T. R. Meyer, S. Roy, T. N. Anderson, J. D. Miller, V. R. Katta, R. P. Lucht, and J. R. Gord, "Measurements of OH mole fraction and temperature up to 20 kHz by using a diode-laser-based UV absorption sensor," Appl. Opt. **44**, 6729-6740 (2005).
8. X. Zhou, J. B. Jeffries, and R. K. Hanson, "Development of a fast temperature sensor for combustion gases using a single tunable diode laser," App. Phys. B **81**, 711-722 (2005).
9. R. M. Mihalcea, D. S. Baer, and R. K. Hanson, "Diode laser sensor for measurements of CO, CO_2, and CH_4 in combustion flows," Appl. Opt. **36**, 8745-8752 (1997).
10. A. Boschetti, D. Bassi, E. Iacob, S. Iannotta, L. Ricci, and M. Scotoni, "Resonant photoacoustic simultaneous detection of methane and ethylene by means of a 1.63-µm diode laser," Appl. Phys. B **74**, 273-278 (2002).
11. X. Liu, X. Zhou, J. B. Jeffries, and R. K. Hanson, "Experimental study of H_2O spectroscopic parameters in the near-IR (6940-7440 cm(-1)) for gas sensing applications at elevated temperature," J. Quant. Spectrosc. Radiat. Transf. **103**, 565-577 (2007).
12. L. A. Kranendonk, R. J. Bartula, and S. T. Sanders, "Modeless operation of a wavelength-agile laser by high-speed cavity length changes," Opt. Express **13**, 1498-1507 (2005).
13. P. V. Kelkar, F. Coppinger, A. S. Bhushan, and B. Jalali, "Time-domain optical sensing," Electron. Lett. **35**, 1661–1662 (1999).
14. L. A. Kranendonk, R. Huber, J. G. Fujimoto, and S. T. Sanders, "Wavelength-agile H_2O absorption spectrometer for thermometry of general combustion gases," Proc. Combust. Inst. **31**, 783-790 (2007).
15. A. R. Alfano ed., *The Supercontinuum Laser Source, 2nd ed.* (Springer, New York, 2006).

16. J. Chou, Y. Han, and B. Jalali, "Time-Wavelength Spectroscopy for Chemical Sensing," IEEE Photon. Technol. Lett. **16**, 1140-1142 (2004).
17. S. T. Sanders, "A wavelength-agile source for broadband sensing," Appl. Phys. B **75**, 799–802 (2002).
18. J. W. Walewski and S. T.Sanders, "High-resolution wavelength-agile laser source based on pulsed super-continua," Appl. Phys. B **79**, 415-418 (2004).
19. M. N. Islam, G. Sucha, I. Bar-Joseph, M. Wegener, J. P. Gordon, and D. S. Chemla, "Broad bandwidths from frequency-shifting solitons in fibers," Opt. Lett. **14**, 370-372 (1989).
20. J. W. Walewski, J. A. Filipa, C. L. Hagen, and S. T. Sanders, "Standard single-mode fibers as convenient means for the generation of ultrafast high-pulse-energy super-continua," Appl. Phys. B **83**, 75-79 (2006).
21. J. Hult, R. S. Watt, and C. F. Kaminski, "Dispersion measurement in Optical Fibres using supercontinuum pulses," J. Lightwave Technol. **25**, 820-824 (2007).
22. G. Hartung, J. Hult, and C. F. Kaminski, "A flat flame burner for the calibration of laser thermometry techniques," Meas. Sci. Technol. **17**, 2485-2493 (2006).
23. L. S. Rothman, D. Jacquemarta, A. Barbe, *et al*., "The HITRAN 2004 molecular spectroscopic database," J. Quant. Spectrosc. Radiat. Transfer **96,** 139-204 (2005).
24. J. Verspecht and K. Rush, "Individual characterization of broadband sampling Oscilloscopes with a nose-to-nose calibration procedure," IEEE Trans. Instrum. Meas. **43**, 347-354 (1994).
25. M. T. McCulloch, E. L. Normand, N. Langford, G. Duxbury, and D. A. Newnham, "Highly sensitive detection of trace gases using the time-resolved frequency downchirp from pulsed quantum-cascade lasers," J. Opt. Soc. Am. B **20**, 1761-1768 (2003).

1. Introduction

Tunable broadband light sources are desirable for many gas sensing applications. This is particularly true in the near-infrared (IR) spectral region, where many gaseous species of interest for chemical processes or atmospheric applications have vibrational overtone transitions. Absorption based sensing with near-IR diode lasers has successfully been employed in a wide variety of combustion, process and pollutant monitoring applications [1-3]. Wide laser tuning ranges allow the simultaneous measurement of spectra of multiple species. Furthermore, the ability to measure a large number of lines for each species also leads to reduced cross-species interference, and allows gas temperatures to be inferred from the relative strengths of lines. The wavelength tuning rate should be fast on the timescales of the process studied. In turbulent combustion processes, for example, typical timescales range from microseconds to milliseconds. Whereas gas sensing has been demonstrated using diode lasers both at high repetition and tuning rates [4-8] or over wide spectral ranges [9-11], there have been very few reports on combining wide bandwidth tuning with very high tuning rates using diode laser technology [12]. This has sparked an increased interest in the use of alternative light sources, such as dispersed supercontinuum sources [13] or Fourier-domain mode-locked lasers [14].

Broadband supercontinuum radiation, with spectral widths exceeding 1000 nm, can be conveniently generated by launching intense pico- or femto-second laser pulses into optical fibres [15]. Rapid wavelength sweeps can be achieved by sending the short pulses through a highly dispersive element, such as a long fibre. In this fashion broad-band spectra can be recorded at high repetition-rates through detection in the time domain [13,16-18]. The spectral resolution of such a measurement is determined by the amount of dispersion employed and by the electronic bandwidth of the detection system.

In this paper we describe the construction and application of an absorption spectrometer based on a supercontinuum generated by launching ps pulses into conventional single-mode fibre. It features a spectral resolution of around 40 pm, which is an improvement over previously reported designs [13, 16-18]. As the spectral resolution is comparable to the width of molecular spectral lines at atmospheric pressure, it permits quantitative measurements of gas concentration to be performed. Spectra covering several hundred nanometers in bandwidth, can be recorded at repetition rates exceeding 1 MHz. We report what we believe is the first use of such a dispersed supercontinuum source for quantitative high-speed gas monitoring. Broadband spectra of CH_4 (1620 nm to 1700 nm) are recorded and used for CH_4 concentration tracking at rates exceeding 100 kHz in order to demonstrate the technology. The

effect of spectral averaging which improves the signal-to-noise ratios but reduces temporal resolution is evaluated, in particular in relation to measurement precision.

2. Experimental apparatus

The experimental set-up employed for the supercontinuum based absorption measurements is illustrated in Fig. 1. Broadband supercontinuum radiation was generated by launching intense picosecond pulses into a 10 m long single-mode fibre (Corning, SMF28). Normally a photonic crystal fibre is employed for this purpose [15], however, efficient spectral broadening can be achieved in a conventional single-mode fibre by employing sufficiently high pulse energies [19, 20]. The pump laser (Fianium, FemtoPower 1060) was a passively mode-locked ytterbium fibre laser emitting 5 ps long pulses at a centre wavelength of 1064 nm. An acousto-optic pulse picker allowed the repetition rate to be varied between 0.3 MHz and 20 MHz. For the experiments reported here a repetition rate of 1.133 MHz was employed, which is the highest repetition rate at which the generated dispersed supercontinuum sweeps remain temporally separated. At this repetition rate the average output power was around 0.82 W, corresponding to a pulse energy of around 0.72 µJ. The pulse energy of the generated supercontinuum was around 0.23 µJ, corresponding to a launching efficiency of around 30%.
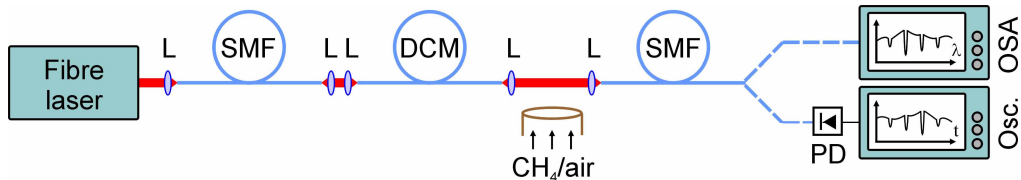

Fig. 1.Experimental set-up for the time-resolved supercontinuum based absorption measurement (L=lens, SMF=single mode fibre, DCM=dispersion compensating module, PD=photo-diode, Osc=oscilloscope, OSA=optical spectrum analyzer).

The spectral profile of the generated supercontinuum radiation extending over more than 700 nm, is shown in Fig. 2. The pump wavelength is located in the normal dispersion regime of the SMF28 fibre, which features a zero-dispersion wavelength (ZDW) of 1312 nm. The supercontinuum is seen to cover the spectral region stretching from 1300 nm to 1700 nm, which is a region of interest for near-IR absorption spectroscopy of a large number of small molecules. The intensity is seen to decrease from about 100 pJ/nm at 1300 nm, to about 6 pJ/nm at 1700 nm. The apparent ripple around 1400 nm is due to absorption by water vapour present in the optical spectrum analyzer (OSA) used for the spectral characterization.
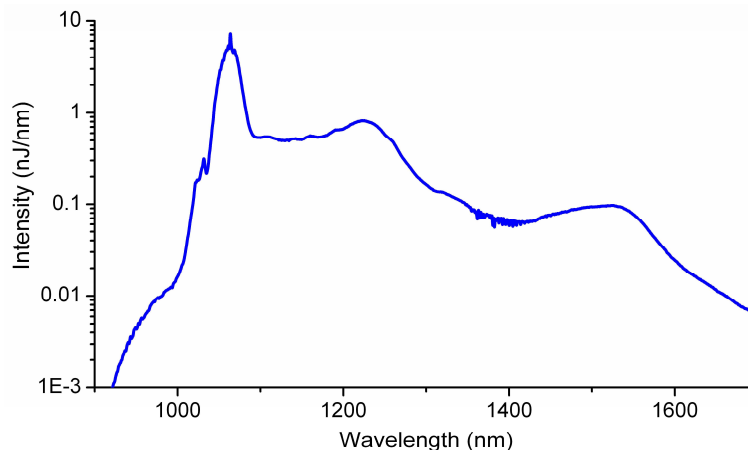

Fig. 2. Spectral profile of the supercontinuum radiation generated in the single-mode fibre (pump pulse energy: 0.85 µJ, pump pulse centre wavelength: 1064 nm).

The broadband supercontinuum pulses were then launched into a second fibre, via free-space coupling. This creates the rapid wavelength sweeps, as different spectral components of the pulse travel through the fibre at different group velocities. The fibre employed for this purpose was a dispersion compensating module (DCM), featuring large negative dispersion (Fujikura, G652-C+L-band SC-DCFM). The dispersion characteristics of the fibre, measured using a novel time-of-flight technique developed by the authors [21], are shown in Fig. 3(a). The absolute value of the dispersion is seen to increase from 0.9 ns/nm at 1300 nm to 2.2 ns/nm at 1650 nm, which causes the output from the DCM to sweep from 1300 nm to 1700 nm in approximately 600 ns. The spectral transmission characteristics of the DCM are shown in Fig. 3(b). The peak transmission, around 1600 nm, is about 18% (7.5 dB), and drops to about 3% (15 dB) at 1300 nm and 1750 nm. The pulse energy after the DCM was around 4 nJ, and covered a spectral width of about 600 nm.
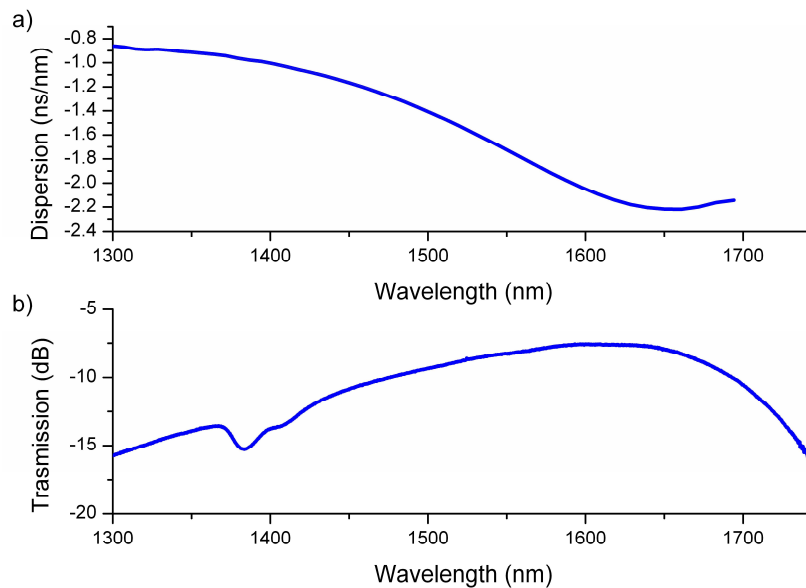

Fig. 3. Experimentally determined a) dispersion curve and b) transmission curve of the dispersion compensating module employed for turning the supercontinuum pulse into a wavelength sweep.

The dispersed supercontinuum pulse, exiting the DCM, is then collimated before passing through the measurement region, and is finally launched back into a single-mode fibre again. The transmitted intensity is detected by a 10 GHz bandwidth preamplified photodiode (Terahertz Technologies, TIA-3000). The photodiode output is finally digitized using a 8 GHz bandwidth real-time oscilloscope (Tektronix, TDS6804B, 20 GS/s), making it possible to observe and store a large number of individual wavelength sweeps. Absorption spectra were also recorded with higher spectral resolution, using an OSA operating at a resolution of around 15 pm (Yokogawa, AQ6317C).

For the absorption measurements presented here the test object consisted of the unburnt CH_4/air gas mixture (about 20% CH_4) exiting a flat flame burner [22]. The burner featured two concentric burner plates, providing a homogeneous CH_4/air stream surrounded by a co-flow of air. A multi-pass arrangement was employed to provide an effective path length of around 10.5 cm through the unburnt gas mixture.

3. Results and discussion

Figure 4 shows a temporal intensity profile recorded by the photodiode and oscilloscope as the dispersed supercontinuum is passed through a CH_4/air mixture. The transmitted intensity

is shown as a function of arrival time at the detector. The instantaneous wavelength, which is determined using the DCM dispersion curve shown in Fig. 3(a), is indicated at the top of the figure. Due to the negative dispersion of the DCM the longest wavelengths arrive first at the detector. The spectral width of the dispersed supercontinuum is around 600 nm, and this range is scanned in only 800 ns. The width of the dispersed supercontinuum is limited by the transmission curve [Fig. 3(b)] of the DCM, however, the exact spectral envelope is also determined by the spectral envelope of the supercontinuum (Fig. 2), the spectral response of the photodiode (which decreases rapidly above 1700 nm), and the wavelength dependence of both beam collimation and fibre launching efficiencies for the broadband supercontinuum beam.

Two sets of absorption lines are clearly seen in the transmission trace. The first group of peaks, extending from 1620 nm to 1700 nm, corresponds to the P-, Q-, and R-branches of the $2v_3$ vibrational overtone transition in CH_4. The second group of peaks, extending from 1350 nm to 1420 nm corresponds to overtone transitions in H_2O. This water absorption is caused by the water vapour present in both the air supplied to the burner and the surrounding ambient air. The trace shown in Fig. 4 corresponds to an average of 1000 wavelength sweeps, for which the total acquisition time was around 0.9 ms. The ripple observed above 1500 nm, which has a period of around 3.5 nm, is thought to be caused by weak etalon effects.
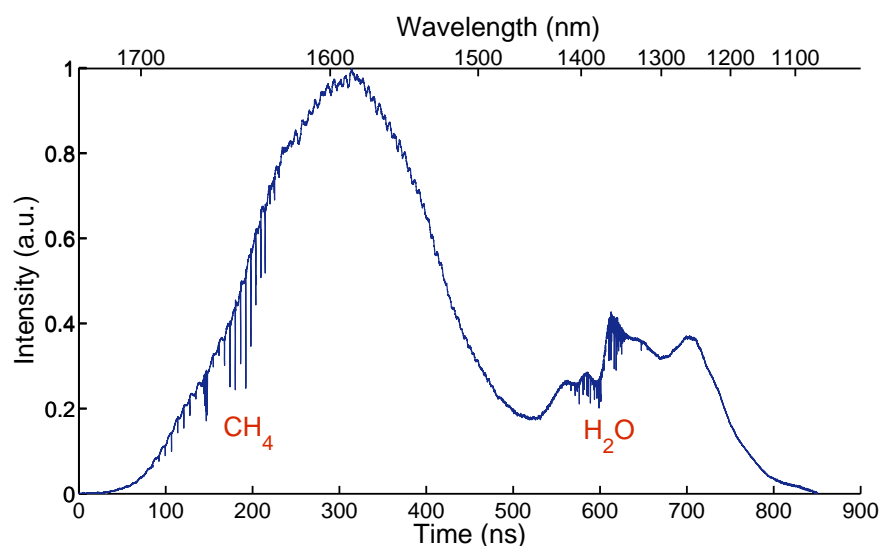

Fig. 4. Intensity of the dispersed supercontinuum pulse, transmitted through a CH_4/air mixture. The absorption peaks around 1650 nm correspond to CH_4 and around 1400 nm to H_2O.

The transmitted intensity in the region covering the CH_4 absorption lines is shown in Fig. 5(a), where the solid line corresponds to an average of 1000 wavelength scans. The fluctuations in intensity are indicated by the shaded area in the background, which corresponds to the standard deviation of the intensity profile. The fluctuations in the intensity profile are observed to be quite large, with a relative standard deviation of around 50% at the centre of the spectrum. The corresponding absorbance spectrum can be calculated from the transmitted radiation, by fitting a baseline to the experimental spectrum shown in Fig. 5(a). The resulting absorbance spectrum, is shown in Fig. 5(b). For this averaged spectrum the observed signal-to-noise ratio was around 190 for the strongest peak in the R-branch and around 80 for the strongest peak in the P-branch. The signal-to-noise ratio is thus relatively good considering that an 80 nm wide spectrum, covering almost the entire P-, Q-, and R-branches, was recorded in less than a millisecond. The spectral resolution of the dispersed supercontinuum absorption measurement is around 39 pm in this spectral region, which is close to the actual width of the CH_4 lines, which is around 38 pm at atmospheric pressure and room temperature. The

experimental resolution is determined by the dispersion of the DCM, which is around -2.2 ns/nm at 1650 nm, and the electronic bandwidth of the detection system. The apparatus function of the detection system was determined by illuminating the photodiode with the pump laser pulses, which have a duration of 5 ps. The full width at half maximum (FWHM) of the apparatus function was measured to be around 85 ps.
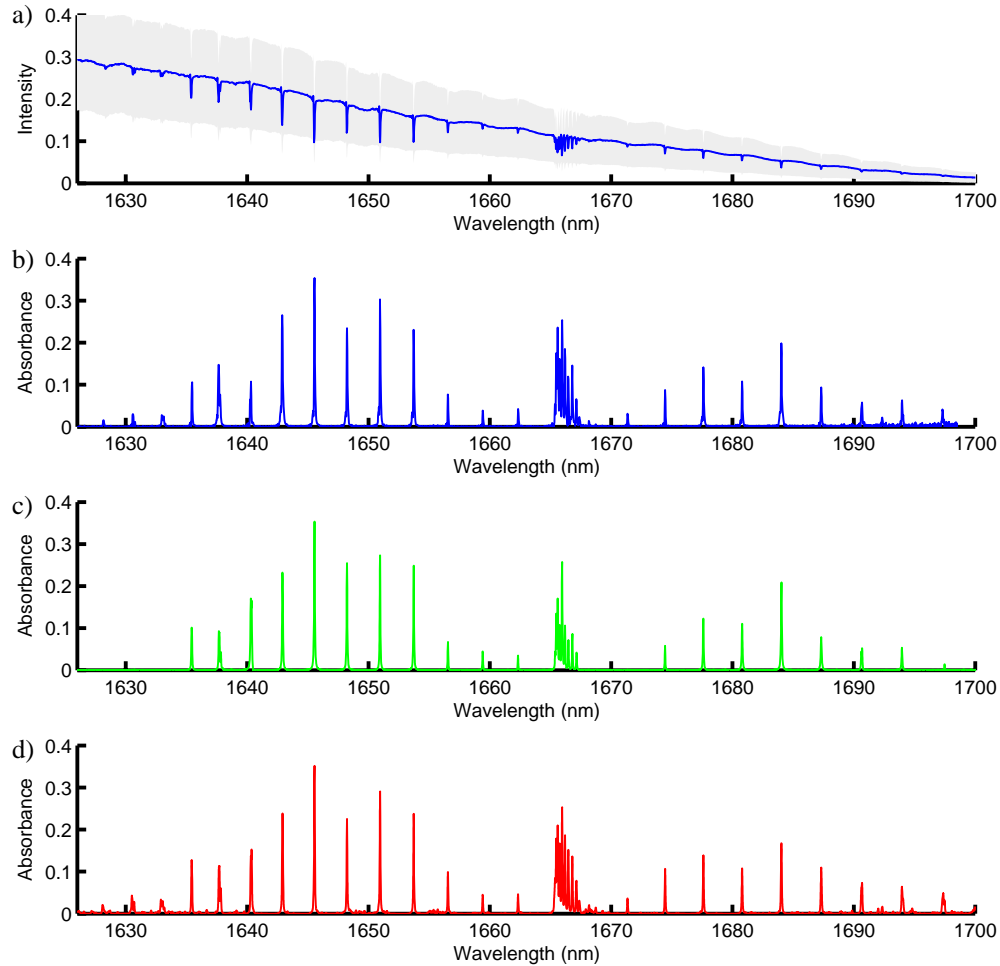

Fig. 5. (a) Intensity of the dispersed supercontinuum pulse transmitted though a CH_4/air mixture, detected using the oscilloscope. The solid line corresponds to an average of 1000 wavelength scans, and the standard deviation of the transmitted intensity is indicated by the shaded area. (b) Experimental CH_4 absorbance spectrum, recorded using the oscilloscope. The acquisition time for this 80 nm wide spectrum was 0.9 ms. (c) The corresponding spectrum measured using an OSA, featuring a spectral resolution of 15 pm. (d) A theoretical spectrum, based on line parameters for CH_4 obtained from the HiTran database, calculated at the experimental pressure (1 atmoshpere) and temperature (296 K). Both the OSA and HiTran spectra were convolved with Gaussian kernels (FWHM=36 pm and FWHM=39 pm, respectively) to match the resolution of the time resolved measurement in b).

The same CH_4 absorption spectrum was also recorded using an OSA for detection, see Fig. 5(c). As this is a scanned grating spectrometer, the acquisition time for the entire spectrum is more than 5 orders of magnitude longer (around 170 s). The spectral resolution of the OSA is around 15 pm, approximately three times better than that of the dispersed supercontinuum measurement. To allow a direct comparison between the two spectra, the spectrum recorded

using the OSA was convolved with a Gaussian filter (FWHM=36 pm) to yield the same spectral resolution. The two spectra are seen to agree reasonably well.

A calculated spectrum, corresponding to the same conditions as in the experiment is shown in Fig. 5(d). Line strength and line shape data were taken from the HiTran 2004 database [23]. The HiTran spectrum has been convolved with a Gaussian filter, the width of which (FWHM=39 pm) corresponds to the experimentally determined spectral resolution of the absorption measurement. Figure 6 shows a fit of two of the measured spectral lines in the R-branch with the HiTran spectrum, and good agreement is seen. The absorption peaks acquired using the dispersed supercontinuum all feature a small side lobe on the low wavelength side. This is an artefact caused by a small oscillation after the main peak in the apparatus function of the detection system, as will be discussed later on.
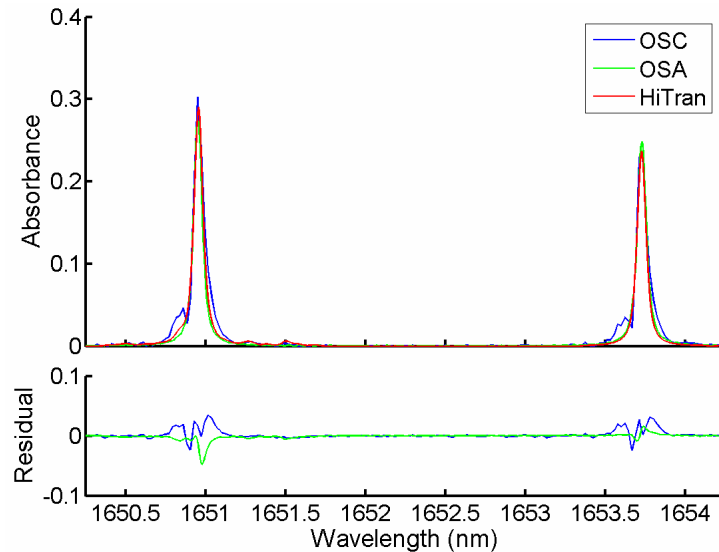

Fig. 6. (1.8 MB). Movie showing a magnified view of the R-branch lines of the $2\nu_3$ transition in CH_4.

The CH_4 concentration was determined from the measured absorption spectra by fitting the strength of the individual HiTran peaks, which were calculated at the experimental pressure and temperature, to each of the experimentally measured peaks. The width of each HiTran peak was matched to the width of the corresponding experimental peak, though fitting the width of the Gaussian filter employed for the convolution. This fitting must be performed directly in the transmission spectrum, to conserve area under the transmission curve following the convolution. For each peak the line centre position as well as a 4th order polynomial baseline, were also fitted. Figure 7 shows one of the CH_4 lines, along with the fitted baseline, the fitted convolved HiTran peak, and the original HiTran peak. Once again the distortion of the line shape on the low wavelength side is apparent in the experimental spectrum. This is caused by an oscillation in the impulse response of the detection system, which is clearly seen in the experimentally measured apparatus function shown in the inset of Fig. 7. The observed shape of the impulse response is characteristic of high bandwidth oscilloscopes [24].
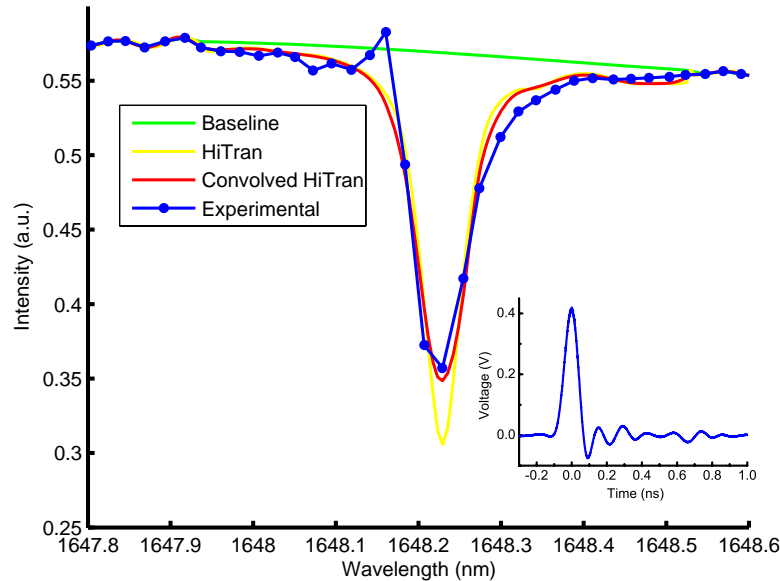
Fig. 7. Magnified view of one of the CH$_4$ absorption peaks visible in the transmission spectrum in Fig. 5(a). The experimental transmission spectrum is shown in blue and the baseline fitted to this curve in green. The corresponding peak calculated using HiTran line parameters at the experimental conditions is shown in yellow. The red trace corresponds to the calculated peak convolved with a Gaussian kernel (FWHM=39 pm) to match the experimental resolution. Inset: Measured impulse response of the detection system.

From the determined intensity scaling factor between each experimental and HiTran peak, the CH$_4$ column density (molecules/m^2) could be determined. For the determination of the column density a weighted average of the peak scaling factors was employed. The relative weight of each peak was determined by its line strength and its baseline intensity, in order to give larger importance to peaks featuring higher signal-to-noise ratios. Finally, the concentration could be determined from the column density by dividing with the path length.

The CH$_4$ column density determined from the spectrum shown in Fig. 5(b) was 5.18×10^{23} m^{-2}, which corresponds to a CH$_4$ concentration of 19.7% in the fuel/air stream, using an estimated value of 10.5 cm for the path length through the open gas stream. This agrees reasonably well with the concentration determined using the rotameters controlling the air and CH$_4$ flow rates, which was 20%. However, a direct comparison is of limited value in the present case, as we estimate that neither the exact path length through the open gas stream nor the flow rates could be determined with accuracies better than a few percent. A more accurate comparison can be made, however, with the column density determined from the CH$_4$ spectrum recorded using the OSA, as this instrument comes close to fully resolving the spectral lines. The column density determined from the OSA spectrum shown in Fig. 5(c) is 5.26×10^{23} m^{-2}, and thus the agreement between the two values is within 1.5%.

The temporal resolution of this type of concentration measurement is determined by the repetition rate of the pump laser and by the number of wavelength scans averaged before each concentration measurement datum is calculated. In the present case the maximum repetition rate of the pump laser is restricted to around 1 MHz, in order to avoid overlapping the blue wing of one spectrum with the red wing of the following spectrum. The amount of averaging, however, is only dependent on the level of precision required. The top pane of the movie in Fig. 8 shows sequentially recorded experimental spectra, corresponding to averages of only 10 wavelength scans. The total acquisition time for each of those spectra was thus only 9 µs, corresponding to a continuous acquisition rate of 113 kHz. This is sufficiently fast to effectively freeze and resolve almost any turbulent or reactive flow process. The bottom pane

shows the time-series of CH_4 column density data determined from the individual spectra. The entire movie sequence covers just over 1 ms, in which time 120 independent concentration measurements are performed. The time series of CH_4 column densities is seen to be stable, with a relative scatter of only 2.6%.
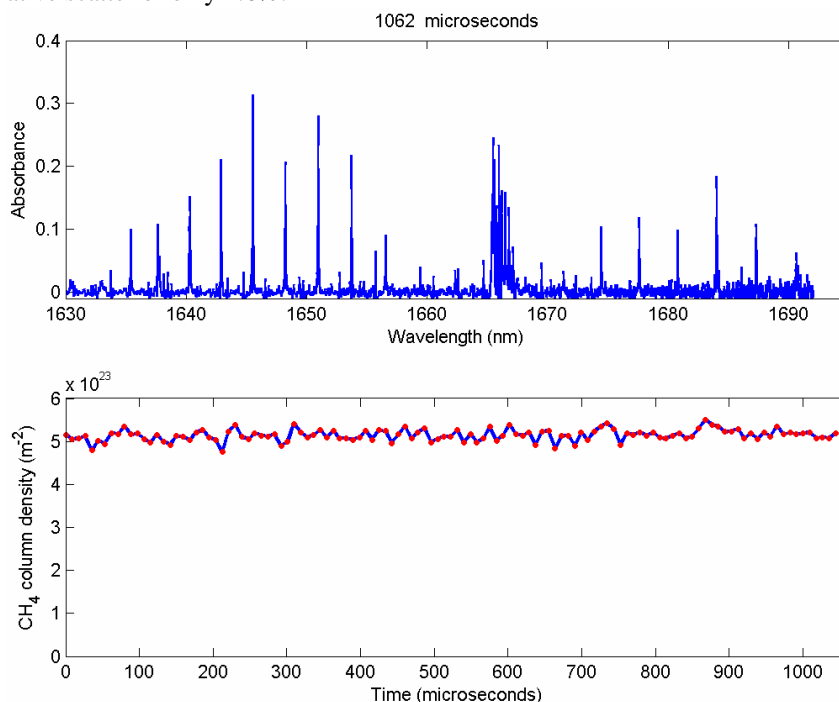

Fig. 8. (1.7 MB). Top: Movie of a continuous sequence of CH_4 absorption spectra, recorded at an acquisition rate of 113 kHz. The laser repetition rate was 1.13 MHz, and each spectrum corresponds to an average of 10 spectra. Bottom: Time series of corresponding measured CH_4 column density.

As the gas flow can be considered stable on such short timescales, the scatter in the evaluated column densities represents the precision of the dispersed supercontinuum measurement. In Fig. 9 the measured column density is shown as a function of the amount of averaging employed, which effectively determines the continuous acquisition rate as the repetition rate of the laser is kept constant. As expected the precision in the measurement decreases with increased acquisition rate, from 0.8% at 5.6 kHz to 2.6% at 113 kHz, as less and less averaging is employed.
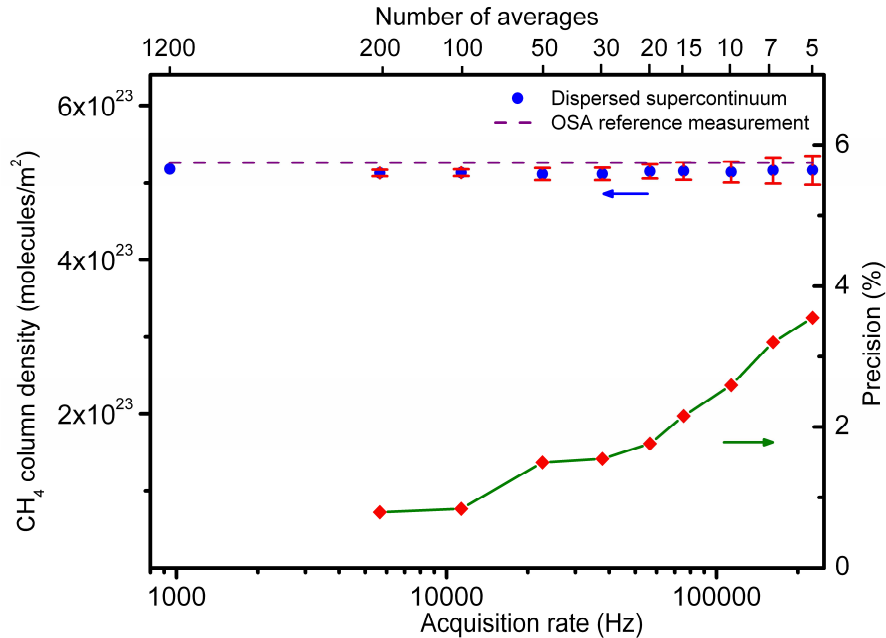
Fig. 9. CH$_4$ column densities measured using the dispersed supercontinuum based absorption measurement technique. Average values and observed standard deviations as a function of the amount of averaging employed are shown. The relative precision is also shown as a function of the acquisition rate.

It is possible to increase the spectral resolution of the absorption measurement by increasing the amount of dispersion employed. In Fig. 10, a CH$_4$ absorption spectrum recorded using two dispersion compensating modules instead of one is shown. The use of two DCMs doubles the dispersion, to around 4.4 ns/nm, resulting in a spectral resolution of around 22 pm. It should be noted that the resolution obtained is close to the fundamental limit set by the uncertainty principle, as the short temporal detection window employed ultimately limits the width of the instantaneous wavelength [25]. The use of dual dispersion modules is particularly valuable for achieving good spectral resolution at shorter wavelengths where the dispersion is lower. At the location of the H$_2$O band shown in Fig. 4, around 1400 nm, the dispersion of a single module is only 1.0 ns/nm, which is about half that of the dispersion in the CH$_4$ region.

As the introduction of a second DCM leads to a reduction of more than 8 dB in laser power, see Fig. 3(b), the signal-to-noise ratio is degraded correspondingly. With the present optical throughput efficiency this forces the use of relatively long averages (1000 scans were used in Fig. 10), thus limiting maximum acquisition rates. It is expected that the use of spliced fibre connections, rather than free-space connections as currently employed, would lead to sufficient improvements in optical throughput to allow the use of double dispersion modules even for high-speed measurements.
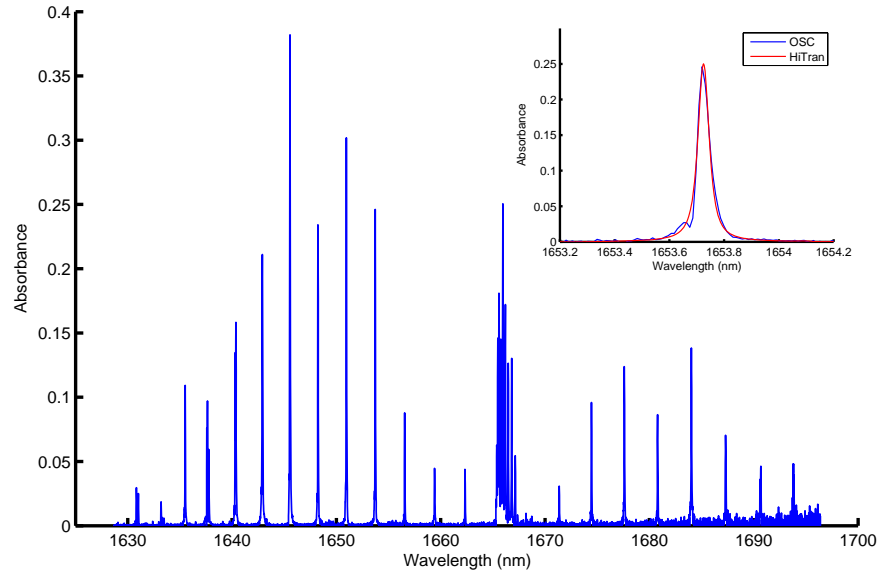
Fig. 10. Experimental CH_4 absorbance spectrum recorded employing a total dispersion of around 4.4 ns/nm, resulting in a spectral resolution or around 22 pm. The spectrum corresponds to an average of 1000 wavelength scans, recorded in 1.8 ms. Insert: Magnified view of one of the experimental CH_4 lines, a theoretical peak (based on HiTran line parameters) is also shown.

4. Conclusion

A dispersed supercontinuum source, capable of acquiring absorption spectra covering hundreds of nanometres at high acquisition rates has been presented. The spectral resolution obtained, 40 pm, is high enough to allow quantitative measurements of gas concentration to be performed at atmospheric pressure conditions. The potential for rapid on-line gas sensing was demonstrated by recording 80 nm wide absorption spectra of the $2v_3$ transition in CH_4, around 1665 nm, at acquisition rates exceeding 100 kHz. From the spectra a quantitative measurement of the CH_4 column density, at the same high repetition-rate, could be made. This work demonstrates the capability of this type of sensor to continuously measure concentrations of major species in gas mixtures, at repetition rates which are fast enough to resolve most dynamic turbulent flow or combustion phenomena.

The use of a direct absorption technique, as employed here, limits the sensitivity possible to obtain. Further development will therefore address the use of either a balanced detection or cavity enhanced scheme to allow lower absorbances to be probed accurately.

The work presented here was focused on the acquisition of spectra in cold flows, whereas current efforts are aimed at extending those capabilities to acquiring spectra of similar quality in reactive flows. This work is motivated by the strong demand for rapid multi-species measurements in many combustion applications, for which dispersed supercontinuum sources show great promise.

Acknowledgments